Available online at www.sciencedirect.com

SCIENCE DIRECT

Physics Letters B 637 (2006) 235–240

PHYSICS LETTERS B

www.elsevier.com/locate/physletb

All-orders resummation for diphoton production at hadron colliders

Csaba Balázs [a], Edmond L. Berger [a], Pavel Nadolsky [a,*], C.-P. Yuan [b]

[a] *High Energy Physics Division, Argonne National Laboratory, 9700 Cass Ave., Argonne, IL 60439, USA*
[b] *Department of Physics and Astronomy, Michigan State University, East Lansing, MI 48824, USA*

Received 13 March 2006; received in revised form 13 April 2006; accepted 13 April 2006

Available online 27 April 2006

Editor: N. Glover

Abstract

We present a QCD calculation of the transverse momentum distribution of photon pairs produced at hadron colliders, including all-orders soft-gluon resummation valid at next-to-next-to-leading logarithmic accuracy. We specify the region of phase space in which the calculation is most reliable, compare our results with data from the Fermilab Tevatron, and make predictions for the Large Hadron Collider. The uncertainty of predictions for production of diphotons from fragmentation of final-state quarks is examined.

PACS: 12.15.Ji; 12.38.Cy; 13.85.Qk

Keywords: Prompt photons; All-orders resummation; Tevatron Run-2 phenomenology

1. Introduction

A Higgs boson with mass between 115 and 140 GeV may be identified at hadron colliders through its decay into a pair of energetic photons, a challenging prospect at the Large Hadron Collider in view of the intense background from hadronic production of non-resonant photon pairs [1]. Theoretical predictions of these background processes may be of substantial value in aiding search strategies. Moreover, the perturbative quantum chromodynamics (QCD) calculation of photon-pair production is of theoretical interest in its own right, and data from the Tevatron collider offer an opportunity to compare and test results against experiment.

In this Letter, we present a new calculation of the diphoton cross section in perturbative QCD. We include contributions from all perturbative subprocesses (quark–antiquark, quark–gluon, antiquark–gluon, and gluon–gluon) to next-to-leading order (NLO) accuracy. In addition, to describe properly the behavior of the transverse momentum Q_T distribution of the pairs in the region in which $Q_T < Q$, where Q is the invariant mass of the photon pair, we include the all-orders resummation of soft and collinear logarithmic contributions up to next-to-next-to-leading log (NNLL) accuracy. This calculation goes beyond the previous resummation treatments of diphoton production [2,3]. Its components are summarized briefly below, and a more complete discussion is presented elsewhere [4].

A full treatment of photon pair production requires that we address the contributions from non-perturbative processes, such as π and η meson decays, and the quasi-collinear fragmentation of quarks and gluons into photons. Elaborate isolation procedures are applied by the experiments to reduce these long-distance contributions, procedures that are only approximately reproducible theoretically. Some final-state fragmentation contributions invariably survive the isolation, especially at the LHC, where the efficiency of isolation is reduced by event pile-up and the large number of energetic hadronic fragments in each event. A new feature of diphoton production, with respect to single photon production, is the prospect that both photons may be produced from fragmentation of the same final-state parton. This fragmentation contribution is expected to be most influential in the region in which both the diphoton invariant mass and the separation $\Delta\varphi$ between the azimuthal angles of the two photons are relatively small, $Q < Q_T$ and $\Delta\varphi < \pi/4$.

* Corresponding author.
E-mail address: nadolsky@hep.anl.gov (P. Nadolsky).

0370-2693
doi:10.1016/j.physletb.2006.04.017

Diphoton production is characterized by large radiative corrections, distributed in a complex pattern over the accessible phase space. The influence of initial-state gluon radiation on the predicted transverse momentum distributions can be evaluated to all orders with the Collins–Soper–Sterman (CSS) resummation procedure [5], the method that we follow. Our results are implemented in a Monte Carlo integration program RESBOS. We use a simple, efficient approximation for the fragmentation contributions. We compare our results with data from the Collider Detector at Fermilab (CDF) Collaboration at $p\bar{p}$ collision energy $\sqrt{S} = 1.96$ TeV and integrated luminosity 207 pb^{-1} [6], and we observe good agreement. We make several suggestions for a further more differential analysis of the data that would allow refined tests of our calculation. In view of theoretical uncertainties associated with the fragmentation component of the cross section, and the presence of other large radiative corrections, we question the conclusion in Ref. [6] that the inclusion of single-photon fragmentation contributions within the NLO calculation of Ref. [7] uniquely explains the observed kinematic distributions of the diphotons at the Tevatron. We also include predictions for diphoton production at the LHC.

2. Analytical calculation

The CSS resummation method is used in Refs. [2,3] to treat the direct production of photon pairs from $q\bar{q}$, $\overset{(-)}{q}g$, and gg scattering. The NLO perturbative cross sections (i.e., cross sections of $\mathcal{O}(\alpha_s)$ in the $q\bar{q}$ and qg channels [8–10], and $\mathcal{O}(\alpha_s^3)$ in the gg channel [3,11–13]) are included as a part of the resummed cross section. Singular logarithms arise in the NLO cross sections when the transverse momentum Q_T of the $\gamma\gamma$ pair is much smaller than its invariant mass Q. These logarithms are resummed into a Sudakov exponent (composed of two anomalous-dimension functions $A(\mu)$ and $B(\mu)$) and convolutions of the conventional parton densities $f_a(x, \mu_F)$ with Wilson coefficient functions C. In Refs. [2,3], the functions $A(\mu)$, $B(\mu)$ and C are evaluated up to order α_s^2, α_s, and α_s, respectively. An approximate expression is used there for the C-function of order α_s in the gg subprocess (borrowed from the $gg \to$ Higgs resummed cross section). In this work, we include the exact C-function of order α_s for $gg \to \gamma\gamma X$ [14] and $\mathcal{O}(\alpha_s^2)$ expressions for $A(\mu)$ and $B(\mu)$ in all subprocesses [14–16]. These enhancements elevate the accuracy of the resummed prediction to the NNLL level. We use an improved model for the non-perturbative contributions at large impact parameter [17]. When expanded in a series in α_s, the resummed predictions for the total rate, $\gamma\gamma$ invariant mass, and $\gamma\gamma$ rapidity (y) distributions are equal to the fixed-order QCD cross sections, augmented by higher-order contributions from the integrated Q_T logs. The resummed Q_T distribution is well-behaved as $Q_T \to 0$, unlike its fixed-order counterpart which is singular in this limit. As Q_T grows, our resummed cross section crosses the perturbative NLO cross section at $Q_T \sim Q$, and, for each Q and y, we switch from the resummed to the NLO cross section for values of Q_T above this point.

A fragmentation singularity arises in the matrix element when the momentum of a photon is collinear with that of an outgoing quark or gluon. The fragmentation singularities do not appear in the resummed terms since those correspond to initial-state radiation. At the lowest order, the fragmentation singularity appears in the $qg \to \gamma\gamma q$ channel and is proportional to $P_{\gamma\leftarrow q}(z)/(n-4)$ in n-dimensional regularization, where $P_{\gamma\leftarrow q}(z)$ is the $q \to \gamma$ splitting function, and z is the fraction of the fragmenting quark's light-cone momentum carried by the photon. The fragmentation singularity is subtracted from the direct contribution. It is resummed in the photon fragmentation function $D_\gamma(z)$ through the introduction of a "one-fragmentation" contribution $q + g \to (q \xrightarrow{\text{frag}} \gamma X) + \gamma$, where "$(q \xrightarrow{\text{frag}} \gamma X)$" denotes collinear production of a photon from a quark. For a wide class of two-to-two partonic processes, such as $q\bar{q} \to q\bar{q}$, etc., there is a second type of "one-fragmentation" contribution that arises in low-mass photon-pair production ($Q < Q_T$). In this case, a final-state parton may fragment into a low-mass pair of photons, a process described by a different fragmentation function $D_{\gamma\gamma}(z_1, z_2)$. This new contribution is not included in the existing calculations. "Two-fragmentation" contributions arise in processes like $g + g \to (q \xrightarrow{\text{frag}} \gamma X) + (\bar{q} \xrightarrow{\text{frag}} \gamma X)$ and involve convolutions with two functions $D_\gamma(z)$ (one per photon).

Isolation constraints must be imposed on the inclusive photon cross sections before the comparison with data. Isolation can be applied to the cross sections at each order of α_s [18–20]. The magnitude of the fragmentation contribution is controlled by the isolation procedure chosen and can be strongly affected by tuning the quasi-experimental isolation model. An isolation condition in a typical measurement requires the hadronic activity to be minimal (e.g., comparable to the underlying event) in the immediate neighborhood of each candidate photon. Candidate photons may be rejected because of energy deposit nearby in the hadronic calorimeter, which introduces dependence on the calorimeter cell geometry, or because hadronic tracks are present near the photons. A theory calculation may approximate the experimental isolation by requiring the full energy of the hadronic remnants to be less than a threshold "isolation energy" E_T^{iso} in the cone $\Delta R = \sqrt{\Delta\eta^2 + \Delta\varphi^2}$ around each photon, with $\Delta\eta$ and $\Delta\varphi$ being the separations of the hadronic remnant(s) from the photon in the plane of pseudo-rapidity η and azimuthal angle φ. The two photons must also be separated in the η–φ plane by an amount exceeding the approximate angular size $\Delta R_{\gamma\gamma}$ of one calorimeter cell. The values of E_T^{iso}, ΔR, and $\Delta R_{\gamma\gamma}$ serve as crude characteristics of the actual measurement. The size of the fragmentation contributions depends tangibly on the assumed values of E_T^{iso}, ΔR, and $\Delta R_{\gamma\gamma}$, as is shown below.

We find it sufficient in our work to use a simplified fragmentation model to represent the isolated cross section. We regularize the fragmentation region by imposing a combination of a sharp cutoff E_T^{iso} on the transverse energy E_T of the final-state quark or gluon and smooth cone isolation [21]. We impose quasi-experimental isolation by rejecting an event if (a) the separation $\Delta r = \sqrt{(\eta - \eta_\gamma)^2 + (\varphi - \varphi_\gamma)^2}$ between the final-state parton and one of the photons is less than ΔR, and (b) E_T of the parton is larger than E_T^{iso}. This condi-

tion excludes the singular fragmentation contributions in the finite-order qg cross section at $\Delta r < \Delta R$ and $E_T > E_T^{\rm iso}$. The fragmentation contributions at $\Delta r < \Delta R$ and $E_T < E_T^{\rm iso}$ are suppressed by rejecting events in the ΔR cone that satisfy $E_T < \chi(\Delta r)$, where $\chi(\Delta r)$ is a smooth function satisfying $\chi(0) = 0$, $\chi(\Delta R) = E_T^{\rm iso}$. This "smooth cone isolation" [21] transforms the non-integrable fragmentation singularity associated with $D_\gamma(z)$ into an integrable singularity of a magnitude dependent on the functional form of $\chi(\Delta r)$. Infrared safety of the cross sections is preserved as a result of smoothness of $\chi(\Delta r)$. The cross section for direct contributions is rendered finite by this prescription without the explicit introduction of fragmentation functions $D_\gamma(z)$. For our smooth function, we choose $\chi(\Delta r) = E_T^{\rm iso}(1-\cos\Delta r)^2/(1-\cos\Delta R)^2$. Modifications to the function $\chi(\Delta r)$ lead to only mild variations of our predicted Q_T distribution for $Q_T < E_T^{\rm iso}$.

In our calculation, we use the electroweak parameters [22] $G_F = 1.16639\times10^{-5}$ GeV^{-2}, $m_Z = 91.1882$ GeV, and $m_W = 80.419$ GeV. We use two-loop expressions for the running electromagnetic and strong couplings $\alpha(\mu)$ and $\alpha_S(\mu)$, as well as the NLO parton distribution function set CTEQ6M [23] and set 1 of the NLO photon fragmentation functions from Ref. [24]. Our choices of the renormalization and factorization scales are the same as in Ref. [2]; in particular, we set $\mu_R = \mu_F = Q$ in the finite-order perturbative expressions.

In impact parameter (b) space, used in the CSS resummation procedure, we must integrate into the non-perturbative region of large b. Contributions from this region are known to be suppressed at high energies [25], but it is important nevertheless to evaluate the expected residual uncertainties. We use a model for the non-perturbative contributions ("revised b_* model") based on the analysis of Drell–Yan pair and Z boson production in Ref. [17]. A non-perturbative Sudakov function for the factorization constant $C_3 = 2e^{-\gamma_E} \approx 1.123$ is used here to describe the non-perturbative terms in the leading $q\bar{q} \to \gamma\gamma$ channel [17]. We neglect possible corrections to the non-perturbative contributions arising from the final-state soft radiation in the qg channel, as well as additional $\sqrt{s}$ dependence affecting Drell–Yan-like processes at $x \lesssim 10^{-2}$ [26], as those exceed the accuracy of the present measurements at the Tevatron. The non-perturbative function in the $gg \to \gamma\gamma$ channel is approximated by multiplying the non-perturbative function for the $q\bar{q}$ channel by the ratio $C_A/C_F = 9/4$ of the color factors $C_A = 3$ and $C_F = 4/3$ for the leading soft contributions in the gg and $q\bar{q}$ channels. Comparing our results based on the "revised b_* model" with those obtained with the original b_* approach, we find at most 10% differences in our predicted $d\sigma/dQ_T$ at the lowest values of Q_T at the Tevatron collider energy, and smaller differences at larger values of Q_T, all well within the experimental uncertainties. The differences are even smaller at the LHC energy [4].

3. Comparison with Tevatron data

Our analysis provides a calculation of the triple-differential cross section $d\sigma/dQ\,dQ_T\,d\Delta\varphi$. Its relevance is especially pertinent for the transverse momentum Q_T distribution in the region $Q_T \leqslant Q$, for fixed values of diphoton mass Q. It would be best to compare our multi-differential distribution with experiment, but the published collider data tend to be presented in the form of single-differential distributions in Q, Q_T, and $\Delta\varphi$, after integration over the other variables. We follow suit in order to make comparisons with the Tevatron collider data, but we comment on the features that can be explored if more differential studies are made. In accord with CDF, we impose the cuts $|y_\gamma| < 0.9$ on the rapidity of each photon, and $p_T^\gamma > p_{T\,\rm min}^\gamma = 14$ (13) GeV on the transverse momentum of the harder (softer) photon in each $\gamma\gamma$ pair. We choose $E_T^{\rm iso} = 1$ GeV, $\Delta R = 0.4$, and $\Delta R_{\gamma\gamma} = 0.3$, unless stated otherwise.

The invariant mass (Q) distribution is shown in Fig. 1(a). It exhibits a characteristic lower kinematic cutoff at $Q \approx 2\sqrt{p_{T\,\rm min}^{\gamma_1} p_{T\,\rm min}^{\gamma_2}} \approx 27$ GeV. Our calculation (RESBOS) agrees well with the data. In this figure we also show the perturbative QCD contributions evaluated at a finite order, represented by the DIPHOX code [7]. Unless specified otherwise, the scales $\mu_R = \mu_F = Q$ are used to obtain the DIPHOX results presented here. The overall agreement between the two calculations is anticipated, since both evaluate the inclusive rates at NLO accuracy. The differences are due to different isolation prescriptions, resummation of higher-order logarithms as well as NLO contributions to the gg channel in our calculation, single-photon and one- and two-fragmentation contributions in DIPHOX.

The transverse momentum (Q_T) distribution of diphotons is shown in Fig. 1(b). The finite-order calculation, represented here by DIPHOX, displays an unphysical logarithmic singularity as $Q_T \to 0$. In our work, the initial-state small-Q_T singularities are resummed in the CSS formalism, resulting in a reasonable overall shape of the cross section at any Q_T. The fragmentation contributions exhibit a double-logarithmic singularity when Q_T approaches $E_T^{\rm iso}$ from below [7], as it is evident in the DIPHOX Q_T distribution for $E_T^{\rm iso} = 4$ GeV. No such singularity is present in our Q_T distribution, which instead has a mild discontinuity at the point $Q_T = E_T^{\rm iso}$ where we switch from the quasi-experimental to smooth-cone isolation.

For the same value $E_T^{\rm iso} = 1$ GeV, our distributions and those of DIPHOX agree well at large Q_T, as a result of our smooth matching of the resummed cross section to the NLO cross section. In the two highest-Q_T bins, the CDF central values lie above the two theory predictions. While the observed excess of events in this "shoulder" region is not significant compared to the present experimental errors, it has been discussed as a possible indication of enhanced fragmentation contributions in the Tevatron data [6,27].

The parameters in DIPHOX can be adjusted to bring its results into agreement with the data in the shoulder region (cf. the dash–dot curves in Figs. 1(b) and 2(a)). The cross section in that region is enhanced if a smaller factorization scale is used, and if the isolation energy $E_T^{\rm iso}$ is increased. The dash–dot curves in Figs. 1(b) and 2(a) are obtained with $\mu_F = 0.5Q$ and $E_T^{\rm iso} = 4$ GeV, compared to the nominal value of $E_T^{\rm iso} = 1$ GeV in the CDF publication. In the shoulder region, the increase in $E_T^{\rm iso}$ to 4 GeV strongly enhances the DIPHOX cross section to

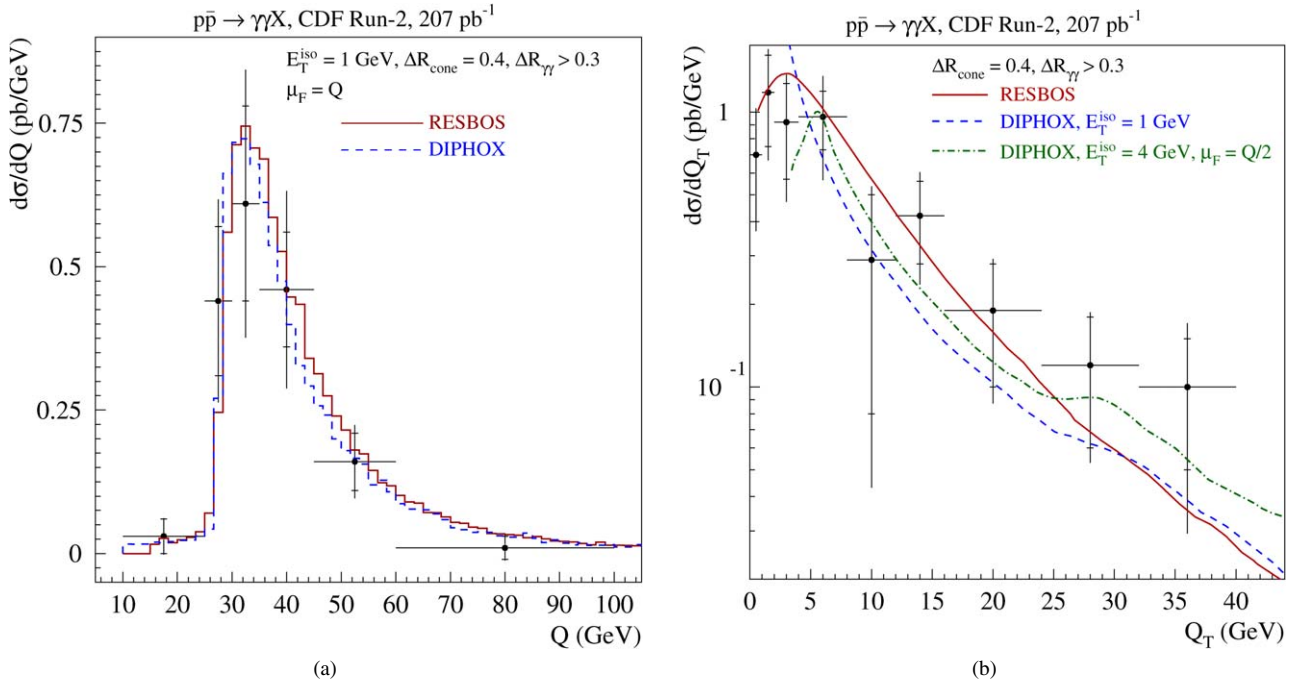

(a) (b)

Fig. 1. (a) Invariant mass and (b) transverse momentum distributions of diphotons. Data from the CDF Run-2 measurement [6] are compared to our calculation (RESBOS) and the DIPHOX calculation.

the value shown in the CDF publication. The magnitude of the one-fragmentation cross section associated with $D_\gamma(z)$ is increased on average by 400% when $E_T^{\rm iso}$ is increased from 1 to 4 GeV.

Our calculations show that most of the shoulder events populate a limited volume of phase space characterized by $\Delta\varphi \lesssim 1$ rad, $Q < 27$ GeV, and $Q_T \gtrsim 25$ GeV. The location of the shoulder in the Q_T distribution is sensitive to the value of the cut on the minimum transverse momentum, p_T^γ, of the individual photons, moving to larger Q_T if these cuts are raised. It has also been noted [27] that non-zero values of $p_T^{\gamma_1}$ and $p_T^{\gamma_2}$ disallow contributions with small Q_T if the azimuthal angle separation between the two photons is small, $\Delta\varphi < \pi/2$. The excess of the experimental rate over our prediction in the region $\Delta\varphi < 0.6$ radian (cf. Fig. 2(a)) contributes the bulk of the excess seen in the shoulder in the Q_T distribution in Fig. 1(b). We note, in addition, that the excess at small $\Delta\varphi$ and large Q_T is characterized by $Q_T \gtrsim Q$.

From a theoretical point of view, when $Q_T > Q$, as in the shoulder region, the calculation must be organized in a different way [28,29] in order to resum contributions arising from the fragmentation of partons into a pair of photons with small invariant mass. In addition, a small azimuthal separation $\Delta\varphi$ often implies that the photons are produced at polar angles $\theta_* \approx 0$ or π in the Collins–Soper diphoton rest frame [30]. The matrix element for the Born scattering process $q\bar{q} \to \gamma\gamma$ diverges as $|\cos\theta_*| \to 1$. Large QCD corrections are known to exist when $|\cos\theta_*| \sim 1$ at any order of the strong coupling strength α_s. Radiation of additional partons at higher orders regularizes the singularity of the quark propagator, yet the enhancement of the cross section is still felt at large $|\cos\theta_*|$. At small Q_T, the $|\cos\theta_*| \approx 1$ contributions are excluded by the cuts $p_T^\gamma > 14$ (13) GeV on the transverse momenta of the individual photons. If, however, the diphoton system is boosted in the transverse direction ($Q_T > Q$), contributions with $|\cos\theta_*| \approx 1$ and substantial rapidity separation $|y_{\gamma_1} - y_{\gamma_2}| > 0.3$ are allowed in the event sample.

Adequate treatment of the light $\gamma\gamma$ pairs and large-$|\cos\theta_*|$ contributions is missing in both our calculation and DIPHOX. The presence of higher-order contributions is reflected in the sensitivity of the DIPHOX prediction at small $\Delta\varphi$ to variations of $E_T^{\rm iso}$, factorization scales, and the angular separation $\Delta R_{\gamma\gamma}$ between the photons [27]. In view of the theoretical uncertainties in the calculation of the fragmentation contributions, and the likely presence of other types of radiative corrections, we suggest that more theoretical and experimental effort is needed to firmly establish the origin of the excess rate in the CDF data at large Q_T and small $\Delta\varphi$, whether from single-photon fragmentation as implemented in DIPHOX or/and other types of enhanced scattering contributions.

The theoretical ambiguities arise in a small part of phase space, where the cross section is also small. Our theoretical treatment is most reliable in the region in which $Q_T < Q$. When the $Q_T < Q$ selection is made, the contributions from $\Delta\varphi < \pi/2$ are efficiently suppressed, and dependence on tunable isolation parameters and factorization scales is reduced (cf. Fig. 2(b)). The fixed-order predictions agree well between our calculation and DIPHOX, while our resummmed cross section also provides an accurate description of the rate at small values of Q_T. After the selection $Q_T < Q$, we expect that the large Q_T shoulder will disappear in the experimental Q_T distribution.

An important prediction of the resummation formalism is a logarithmic dependence on the diphoton invariant mass Q. In

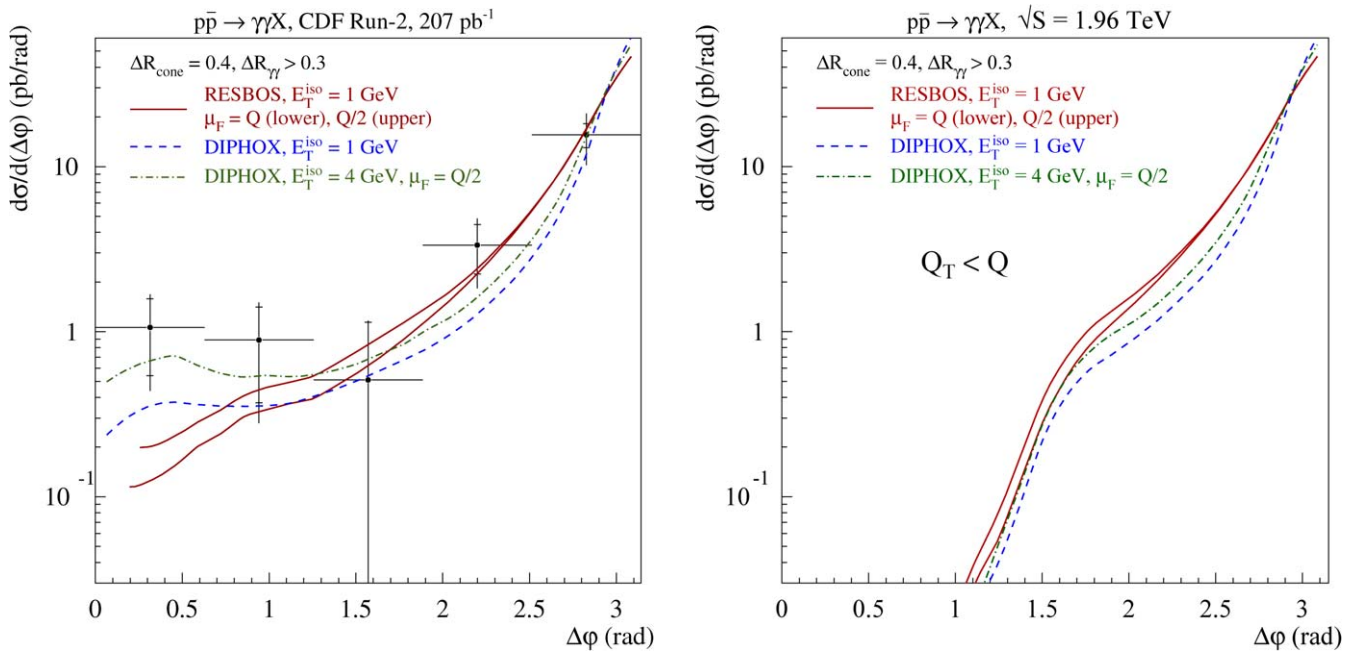

Fig. 2. (a) Distribution over the azimuthal separation $\Delta\varphi$ between the two photons. Data from the CDF Run-2 measurement [6] are compared with our calculation (RESBOS) and the DIPHOX calculation for different isolation parameters; (b) same as (a), with an additional cut $Q_T < Q$ on the diphoton momentum. Our cross sections are evaluated with the factorization scales $\mu_F = Q$ (lower curve) and $0.5Q$ (upper curve) in the finite-order contribution.

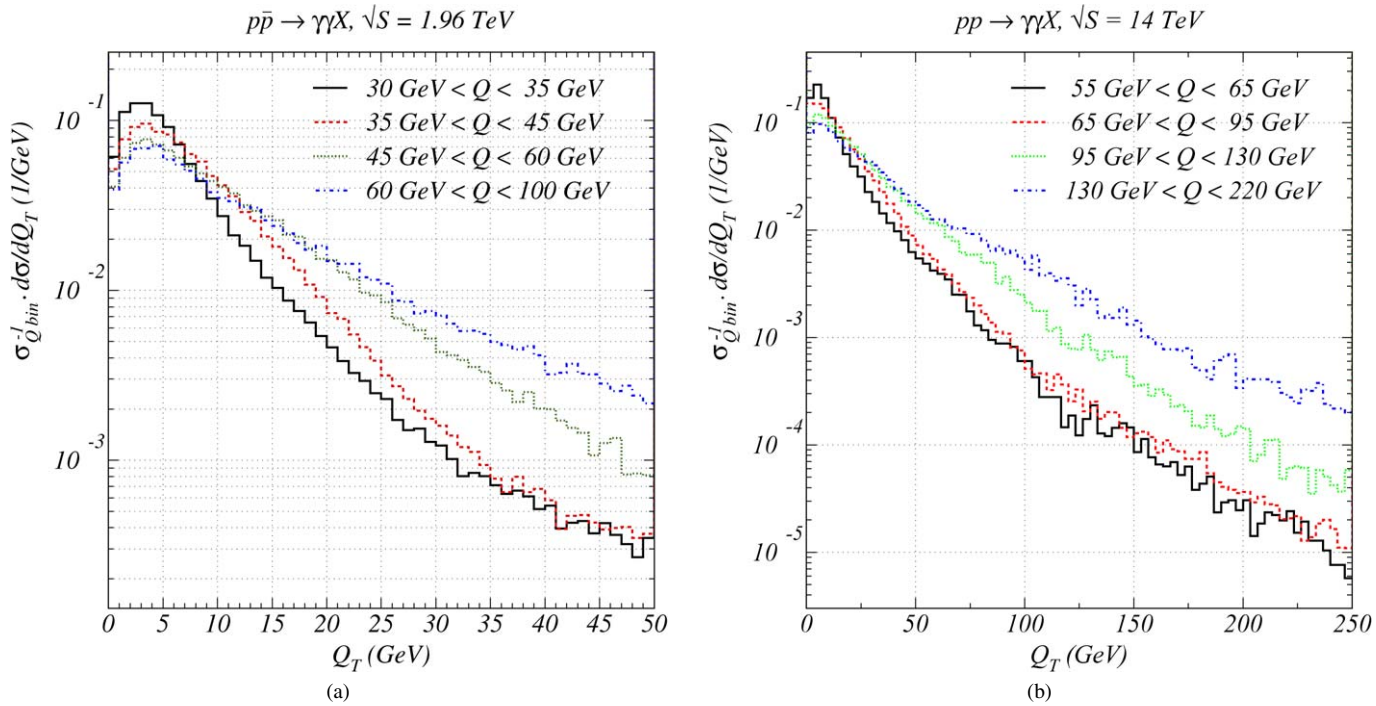

Fig. 3. Resummed transverse momentum distributions of photon pairs in various $\gamma\gamma$ invariant mass (Q) bins at (a) the Tevatron and (b) the LHC. The curves are calculated with the cuts specified in the text. The cross sections are normalized to the total cross section in each bin of Q. We note that our predictions are most reliable in the region $Q_T < Q$, but we plot the curves over the full range of Q_T, using the procedure described in the text to switch from the resummed to the finite-order perturbative results for $Q_T > Q$.

Fig. 3(a), we show the resummed transverse momentum distributions for various intervals of Q. The Q_T distribution is predicted to broaden with increasing Q. The average values of Q_T are $\langle Q_T \rangle = (6.5, 8.1, 10.7, \text{and } 12.6)$ GeV for invariant masses in the intervals (30–35, 35–45, 45–60, and 60–100) GeV, respectively. To compute these averages, we integrate over the range $Q_T = 0$ to 200 GeV. We urge the CDF and D0 Collaborations to verify this predicted broadening with Q.

4. Results for the LHC

To obtain predictions for pp collisions at $\sqrt{S} = 14$ TeV, we employ the following cuts on the kinematics of the individual photons. For each photon, we require transverse momentum $p_T^\gamma > 25$ GeV and rapidity $|y_\gamma| < 2.5$. We impose a somewhat looser isolation restriction than for the Tevatron study, requiring less than $E_T^{\rm iso} = 10$ GeV of extra transverse energy inside a cone with $\Delta R = 0.7$ around each photon.

Fig. 3(b) shows the resummed transverse momentum distributions for various selections of diphoton invariant mass at the LHC. The plot shows the broadening of the Q_T distribution with increasing mass: in the ranges (55–65, 65–95, 95–130, and 130–250) GeV the values of $\langle Q_T \rangle$ are (14, 17, 25, and 33) GeV. At the LHC, we integrate from $Q_T = 0$ to 250 GeV to obtain the averages. For the mass range appropriate in the search for a Standard Model Higgs boson, e.g., 115 to 130 GeV, the diphoton background that we consider in this Letter has $\langle Q_T \rangle \sim 27$ GeV, to be compared with the expectation for the signal of ∼40 GeV [25]. The harder transverse momentum distribution for the signal arises because their is more soft gluon radiation in the dominant gluon-fusion Higgs boson production process [25]. Additional predictions for the LHC are presented in Ref. [4].

5. Summary

We present a new QCD calculation of the transverse momentum distribution of photon pairs produced at hadron colliders, including all-orders resummation of initial-state soft gluon radiation valid at next-to-next-to-leading logarithmic accuracy. This calculation is most appropriate for values of $\gamma\gamma$ transverse momentum Q_T not in excess of the $\gamma\gamma$ invariant mass Q. Resummation changes both the shape and normalization of the Q_T distribution, with respect to a finite-order calculation, in the range of values of Q_T where the cross section is largest. Comparison of our results with data from the Fermilab Tevatron shows good agreement, and we offer suggestions for a more differential analysis of the Tevatron data. We also include predictions for the Large Hadron Collider.

Our calculation accounts for the effects of soft gluon radiation on transverse momentum distributions through all orders of α_s. The NLO calculation with inclusion of single-photon fragmentation [7] is another important approach to $\gamma\gamma$ production. However, theoretical uncertainties are present in the rate of fragmentation contributions associated with the kinematic approximations and tunable parameters in the quasi-experimental isolation condition. For $Q_T > Q$ ($\Delta\varphi < \pi/2$), new types of higher-order contributions are expected to enhance the rate above our predictions. The interpretation of the region of small $\Delta\varphi$ remains ambiguous, as several distinct processes may contribute to the enhanced rate. This interesting region warrants further theoretical investigation. With the contributions from the $Q_T > Q$ region removed, our calculation describes the leading contributions in the $q\bar{q} + qg$ and gg diphoton production channels at NNLL accuracy.

Acknowledgements

We acknowledge helpful discussions with R. Blair, J. Proudfoot, J. Huston, J.-P. Guillet, and Y. Liu. Work at Argonne is supported in part by the US Department of Energy, Division of High Energy Physics, Contract W-31-109-ENG-38. The work of C.P.Y. is supported by the US National Science Foundation under award PHY-0244919. We acknowledge the use of *Jazz*, a 350-node computing cluster operated by the Mathematics and Computer Science Division at ANL as part of its Laboratory Computing Resource Center.

References

[1] ATLAS Collaboration, Atlas detector and physics performance, Technical Design Report, vol. 2, CERN-LHCC-99-15 (unpublished);
CMS Collaboration, The electromagnetic calorimeter project, Technical Design Report No. CERN-LHCC-97-33, 1997 (unpublished).
[2] C. Bálazs, E.L. Berger, S. Mrenna, C.-P. Yuan, Phys. Rev. D 57 (1998) 6934.
[3] C. Bálazs, P. Nadolsky, C. Schmidt, C.-P. Yuan, Phys. Lett. B 489 (2000) 157.
[4] C. Balázs, E.L. Berger, P. Nadolsky, C.-P. Yuan, in preparation.
[5] J.C. Collins, D.E. Soper, G. Sterman, Nucl. Phys. B 250 (1985) 199.
[6] D. Acosta, et al., CDF Collaboration, Phys. Rev. Lett. 95 (2005) 022003.
[7] T. Binoth, J.-P. Guillet, E. Pilon, M. Werlen, Eur. Phys. J. C 16 (2000) 311.
[8] P. Aurenche, A. Douiri, R. Baier, M. Fontannaz, D. Schiff, Z. Phys. C 29 (1985) 459.
[9] E.L. Berger, J. Qiu, Phys. Rev. D 44 (1991) 2002.
[10] B. Bailey, J.F. Owens, J. Ohnemus, Phys. Rev. D 46 (1992) 2018.
[11] D. de Florian, Z. Kunszt, Phys. Lett. B 460 (1999) 184.
[12] Z. Bern, A. De Freitas, L.J. Dixon, JHEP 0109 (2001) 037.
[13] Z. Bern, L.J. Dixon, C.R. Schmidt, Phys. Rev. D 66 (2002) 074018.
[14] P.M. Nadolsky, C.R. Schmidt, Phys. Lett. B 558 (2003) 63.
[15] D. de Florian, M. Grazzini, Phys. Rev. Lett. 85 (2000) 4678.
[16] D. de Florian, M. Grazzini, Nucl. Phys. B 616 (2001) 247.
[17] A.V. Konychev, P.M. Nadolsky, Phys. Lett. B 633 (2006) 710.
[18] E.L. Berger, X.-F. Guo, J. Qiu, Phys. Rev. Lett. 76 (1996) 2234.
[19] S. Catani, M. Fontannaz, E. Pilon, Phys. Rev. D 58 (1998) 094025.
[20] S. Catani, M. Fontannaz, J.-P. Guillet, E. Pilon, JHEP 0205 (2002) 028.
[21] S. Frixione, Phys. Lett. B 429 (1998) 369.
[22] S. Eidelman, et al., Review of Particle Physics, Phys. Lett. B 592 (2004) 1.
[23] J. Pumplin, et al., JHEP 0207 (2002) 012.
[24] L. Bourhis, M. Fontannaz, J.-P. Guillet, Eur. Phys. J. C 2 (1998) 529.
[25] E.L. Berger, J. Qiu, Phys. Rev. D 67 (2003) 034026.
[26] S. Berge, P. Nadolsky, F. Olness, C.-P. Yuan, Phys. Rev. D 72 (2005) 033015.
[27] T. Binoth, J.-P. Guillet, E. Pilon, M. Werlen, Phys. Rev. D 63 (2001) 114016.
[28] E.L. Berger, L.E. Gordon, M. Klasen, Phys. Rev. D 58 (1998) 074012.
[29] E.L. Berger, J. Qiu, X. Zhang, Phys. Rev. D 65 (2002) 034006.
[30] J.C. Collins, D.E. Soper, Phys. Rev. D 16 (1977) 2219.